Process integration of a Ca-looping carbon capture process in a cement plant

International Journal of Greenhouse Gas Control 19 (2013) 530–540

Contents lists available at ScienceDirect

International Journal of Greenhouse Gas Control

journal homepage: www.elsevier.com/locate/ijggc

Process integration of a Ca-looping carbon capture process in a cement plant

Dursun Can Ozcan, Hyungwoong Ahn, Stefano Brandani *

Institute for Materials and Processes, School of Engineering, University of Edinburgh, Mayfield Road, Edinburgh EH9 3JL, UK

ARTICLE INFO

Article history:
Received 10 June 2013
Received in revised form 7 October 2013
Accepted 8 October 2013
Available online 13 November 2013

Keywords:
Carbon capture
Cement plant
Ca-looping process

ABSTRACT

An analysis of the integration of a Ca-looping process into a cement plant is presented. The capture process, based on selective absorption of CO_2 by calcium oxide, has two interconnected reactors where the carbonator captures CO_2 from the preheater flue gases and the calciner regenerates the $CaCO_3$ into CaO by oxy-combustion. The study also considers the purge rate of part of the circulating CaO, given the tendency of the material to sinter and reduce its capture capacity. Fresh $CaCO_3$ is added to maintain reactivity in the carbonator, while the purged sorbents are utilised as a cement kiln feed. The detailed carbonator model has been implemented using Matlab and incorporated into Unisim to provide a full flowsheet simulation for an exemplary dry-feed cement plant as a user-defined operation. The effect of molar flowrate ratio of lime make-up to feed CO_2 (F_0/F_{CO_2}) between two operational limits has been investigated. This process configuration is capable of achieving over 90% CO_2 capture with additional fuel consumption of 2.5–3.0 GJ_{th}/ton CO_2 avoided which depends on the F_0/F_{CO_2} ratio. It is found that a proper heat recovery system supplementary to the Ca-looping process makes the Ca-looping process more competitive than the traditional low temperature absorption process based on amine solvents.

1. Introduction

The cement industry accounts for more than 5% of global CO_2 emission from stationary sources amounting to 1.88 Gt CO_2/year in 2006 (IEA, 2009). It is foreseen that the emissions for the cement sector will continue to grow in parallel with increasing demand of cement (CW Group, 2012) and reach 4.3 Gt CO_2/year until 2050 (WWF, 2008) which is regarded as one of the major industrial carbon emission sources for which it is worth implementing carbon capture and storage solutions. The CO_2 emissions from cement plants originates from different sources; over 50% of the emissions result from the calcination of limestone in the raw material while the rest is generated by fuel combustion (40%) and indirect emissions relating to use of electricity (IEA, 2011). The fuel consumption is significant due to the highly endothermic calcination reaction and high temperature operation in a kiln (around 1450 °C). It has been reported that, with modern technology, the average energy consumption in a cement plant has been reduced to around 2.9 GJ/ton clinker (WBCSD, 2009) and CO_2 emission by calcination can be increased to almost 70% by a more efficient use of the fuel (Rodriguez et al., 2009).

CO_2 emissions in a cement process can be partially reduced by modifications: improving the process for more efficient use of the fuel, replacing fossil fuels with alternative renewables including waste residues, and mixing clinkers with mineral additives (Hasanbeigi et al., 2012). Even though these measures can reduce CO_2 emissions resulting from fuel combustion significantly, they cannot tackle the CO_2 emission originating from the calcination reaction. Therefore, it is essential to deploy a carbon capture technology on cement processes in order to reduce CO_2 emissions by more than 90%.

Several carbon capture technologies including amine scrubbing (IEA, 2008; Hassan, 2005), ammonia scrubbing (Dong et al., 2012), oxy-combustion (IEA, 2008; ECRA, 2009), anti-sublimation (Pan et al., 2013), calcium looping (Bosoaga et al., 2009; Vera, 2009; Rodriguez et al., 2012; Stallmann, 2013) and indirect calcination (Rodríguez et al., 2011a) have received great interest to capture CO_2 from cement industry. The most conventional technology available for carbon capture in a cement plant is a post-combustion amine process. The amine scrubbing (MEA) based post-combustion method has been proposed to reduce CO_2 emissions from a cement plant and shows the possibility to capture the released CO_2 by up to 85% (IEA, 2008; Hassan, 2005). As there is no source of steam available in situ for the regeneration of the amine, unlike in a power plant, there is the need to install a new external steam generator to supply the stripper reboiler of the amine process with low pressure steam while part of the steam requirement can be fulfilled by

* Corresponding author. Tel.: +44 131 6519030.
E-mail address: s.brandani@ed.ac.uk (S. Brandani).

1750-5836/$ – see front matter © 2013 Elsevier Ltd. All rights reserved.
http://dx.doi.org/10.1016/j.ijggc.2013.10.009

Nomenclature

a	decay constant of solid concentration in the lean region (m^{-1})
A_t	cross sectional area of the reactor (m^2)
b	decay constant of contacting efficiency in the lean region (m^{-1})
C_{CO_2*}	equivalent CO_2 concentration in the CFB riser (mol/m^3)
$C_{CO_2,d}$	CO_2 concentration in the dense region exit (mol/m^3)
$C_{CO_2,eq}$	CO_2 concentration allowed by chemical equilibrium (mol/m^3)
$C_{CO_2,in}$	CO_2 concentration in the reactor inlet (mol/m^3)
$C_{CO_2,out}$	CO_2 concentration in the reactor exit (mol/m^3)
d_p	particle diameter (m)
E_{CO_2}	fraction of CO_2 captured to total CO_2 entering the carbonator
f_t	fraction of sorbent particles with a residence time t
F_{ash}	molar flow rate of ash entering the Ca-looping system (kmol/s)
F_0	make-up flow rate (kmol/s)
F_{CO_2}	molar flow rate of CO_2 in a flue gas stream entering the carbonator (kmol/s)
F_R	circulated sorbent flow rate (kmol/s)
F_S	molar flow rate of sulfur entering the Ca-looping system (kmol/s)
H_d	height of the dense region (m)
H_l	height of the lean region (m)
H_t	total height of the carbonator (m)
$k_{ri,ave}$	average kinetic constant of the population of potentially active Ca-based solids (s^{-1})
k_s	rate constant for the carbonation reaction at the surface of CaO ($m^4/mol/s$)
K_{cw}	core-wall mass transfer coefficient (s^{-1})
M_s	molar mass of total solids (kg/kmol)
$M_{s,a}$	molar mass of potentially active Ca-based solids (kg/kmol)
$n_{s,a}$	moles of potentially active Ca-based solids (kmol)
N	number of carbonation/calcination cycles
p	pressure (Pa)
$P_{CO_2,eq}$	equilibrium CO_2 partial pressure (Pa)
r_N	mass fraction of particles after N cycles of carbonation–calcination
S_N	specific surface area available after N cycles of carbonation–calcination (m^2/m^3)
t	time (s)
t_{lim}	time required for a particle to reach its maximum carbonation (s)
T	temperature (K)
T_C	condenser temperature (C)
T_H	superheated steam temperature (C)
u_0	superficial velocity of a gas (m/s)
$V_{g,in}$	volumetric flow rate of inlet gas stream (m^3/s)
$V_{g,out}$	volumetric flow rate of outlet gas stream (m^3/s)
W_s	solid inventory in the carbonator (kg)
x_{ash}	molar fraction of ash
x_{CaSO_4}	molar fraction of $CaSO_4$
X	conversion of CaO to $CaCO_3$
X_{ave}	average carbonation level
$X_{max,ave}$	maximum average carbonation degree of the sorbent after N cycles of carbonation–calcination
$X_{max,N}$	maximum carbonation conversion rate after N cycles of carbonation–calcination

Greek letters

ε_s^*	asymptotic solid volumetric fraction
$\varepsilon_{s,c}$	volume fraction of solids in the lower dense region leaner core zone
$\varepsilon_{s,d}$	volume fraction of solids in the lower dense region
$\varepsilon_{s,e}$	volume fraction of solids at the carbonator exit
$\varepsilon_{s,w}$	volume fraction of solids in the lower dense region denser wall zone
ρ_s	density of total solids (kg/m^3)
$\rho_{s,a}$	density of potentially active Ca-based solids (kg/m^3)
μ	viscosity (kg/m/s)
η_{sd}	the contact efficiency of the dense region
η_T	steam turbine efficiency
δ	the core volumetric fraction of the dense region
ξ	volume ratio between the potentially active solids and the total solids
τ	average residence time of solids particles (s)
ΔX_{CaSO_4}	average fraction of sorbent sulfated at each cycle

Chemical compounds

AS_4H	pyrophyllite
AS_2H_2	kaolinite
C_3S	alite
C_2S	belite
C_3A	tricalcium aluminate
C_4AF	tetracalcium aluminate

the use of hot gases generated in the kiln (Handagama et al., 2013). The steam generator to be deployed could generate some electricity with one back pressure turbine as well as steam (IEA, 2008) but such a steam cycle would have a very low power plant efficiency since it would not be designed with the same complexity as a steam cycle in a purposely designed power plant. Oxy-combustion processes can also be an alternative to the amine capture process. In this case pure oxygen is supplied to the reactor instead of air, so that it is in principle possible to capture CO_2 from the pre-calciner, but there is technical uncertainty in operating a cement kiln under oxy-combustion conditions (IEA, 2008). For that reason, in the IEA (2008), oxy-combustion has not been applied to the cement kiln but only the pre-calciner. Therefore, the overall carbon capture rate is limited since only part of the CO_2 emitted can be captured.

One of the promising technologies for carbon capture from industrial sources is an absorption process based on the reversible reaction of CO_2 on specific metal oxides at high temperature. CaO-based sorbents have attracted the most attention owing to their high absorption capacity, wide availability, and low cost. The post-combustion calcium looping (Ca-looping) process, first proposed by Shimizu et al. (1999), uses a state-of-the-art circulating fluidized bed (CFB) system and offers relatively small energy penalty (Martínez et al., 2011; Zhao et al., 2013). In addition to significant efforts on laboratory scale investigations (Alonso et al., 2010; Charitos et al., 2010; Rodríguez et al., 2011b), several different projects around the world have been initiated to scale up the Ca-looping technology, including a 1.7 MW_{th} pilot plant which has been in operation to demonstrate the concept in La Preda, Spain funded under the "CaOling" project (Arias et al., 2013). Furthermore, promising results have also been reported from 1 MW_{th} pilot plant in Darmstadt (Plötz et al., 2012) and 200 kW_{th} pilot plant in Stuttgart University (Dieter et al., 2012). The Ca-looping process has been proposed as a proper way to reduce CO_2 emissions from power plants (Strohle et al., 2009). One of the greatest challenges related to this method is the deterioration of the CO_2 capture capacity when these materials are used over countless cycles of carbonation

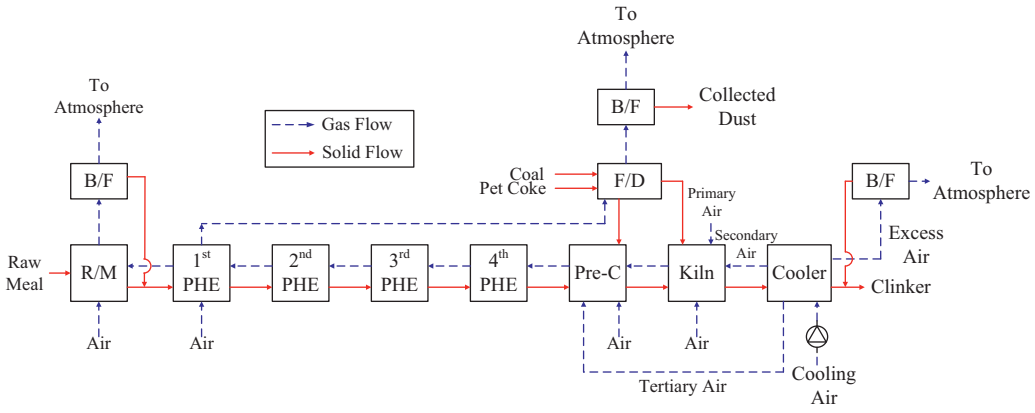

Fig. 1. Schematic diagram of a cement plant without a CO_2 capture unit (base case) (IEA, 2008). Abbreviations: R/M, raw mill; B/F, bag filter; F/D, fuel drying; PHE, preheater; Pre-C, pre-calciner.

and calcination reactions (Curran et al., 1967). Hence, while some spent sorbents are removed as purge from the system, fresh make-up sorbents are introduced. The purge stream from the calciner is mainly composed of CaO with small amounts of $CaSO_4$ and ash. It has already been suggested that the spent CaO from a Ca-looping unit integrated with a power plant can be utilised as feedstock in a cement plant in place of limestone (Dean et al., 2011a). In a later work, it was shown experimentally that cement can be successfully produced from the purge of the Ca-looping process (Dean et al., 2011b). Therefore, it can be envisaged that a significant cut in carbon emission from power and cement plants can be made by process integration between both industries, but colocation is seldom possible. However, it should be noted that the use of purge for clinker production cannot inhibit all CO_2 emission from cement plants since it can only reduce CO_2 emission relating to calcination unless colocation is possible (Romeo et al., 2011). Thus, the potential use of the purge stream in a cement plant leads to an interest in the direct integration of the Ca-looping process with a cement plant. Rodriguez et al. (2012) investigated two alternative process configurations for carbon capture from cement plants. They reported that a retrofit replacing the existing pre-calciner with an oxy-calciner can achieve 89% capture and in addition the capture rate can be improved to up to 99% by capturing CO_2 from the kiln gas using the carbonator. In their study, the carbonator is fed with the mixture of limestone and clay which is preheated by CO_2-rich gas stream leaving the calciner; therefore, there is a need of an air-leakage-free preheater for the production of high purity CO_2.

A novel process configuration having an external combustor to generate heat for the pre-calciner instead of oxy-combustion has been suggested as a way of recovering CO_2 in cement plants (Rodríguez et al., 2011a). This process is capable of producing an enriched-CO_2 stream from the pre-calciner by supplying the heat required for calcination using hot CaO circulating between the combustor and the pre-calciner instead of using the heat of combustion inside the pre-calciner. While this process can capture the CO_2 involved in calcination, it cannot recover the CO_2 generated by fuel combustion. Therefore, this process is a worthwhile option only when a moderate level of CO_2 recovery is required.

In this study, we present a detailed analysis of a typical cement manufacturing process and study the reasonable selection of location of the capture process with respect to process conditions when a Ca-looping process is integrated in a cement plant. Process simulation includes the implementation of a detailed carbonator model and its incorporation into a full cement process simulation.

2. Process simulation of a cement plant (base case)

Fig. 1 shows the block flow diagram of a dry cement process, hereinafter named the base case configuration. The base case includes all the major units in the cement plant: raw mill; preheaters; pre-calciner; kiln and cooler. The base case simulation takes into account key reactions taking place in the process of cement production. Several auxiliary units, such as crushing and milling of the raw materials, cement mixing and milling with fly ash and gypsum are not included in this study since their contribution to the energy balance is not as important as the major units included. In addition, their operations are not affected by retrofitting the carbon capture units into the cement plant. It should be highlighted that the base configuration has a separate pre-calciner upstream of a kiln instead of having a single reactor for calcination and clinkerization since it is well-known that it can provide a lower energy consumption and shorter kiln length (IEA, 2008). The ratio of heat supply into pre-calciner and kiln is maintained at 6 to 4 in this study.

It is crucial to identify the chemical reactions occurring in each unit and determine their conversion rate in order to have accurate mass and energy balances. Table 1 shows the reactions being considered which can be classified into the decomposition of the raw

Table 1
Chemical reactions and their standard enthalpies considered in this cement plant simulation (Taylor, 1990).

Reaction	ΔH (kJ/kg)	Reference
$CaCO_3$ (calcite) → CaO + CO_2(g)	+1782	$CaCO_3$
AS_4H (pyrophyllite) → α-Al_2O_3 + 4SiO_2 (quartz) + H_2O(g)	+224	AS_4H
AS_2H_2 (kaolinite) → α-Al_2O_3 + 2SiO_2 (quartz) + 2H_2O(g)	+538	AS_2H_2
2FeO·OH (goethite) → α-Fe_2O_3 + H_2O(g)	+254	FeO·OH
2CaO + SiO_2 (quartz) → β-C_2S	−734	C_2S
3CaO + SiO_2 (quartz) → C_3S	−495	C_3S
3CaO + α-Al_2O_3 → C_3A	−27	C_3A
4CaO + α-Al_2O_3 + α-Fe_2O_3 → C_4AF	−105	C_4AF
S + O_2 → SO_2	−17,813	S
CaO + SO_2 + 0.5O_2 → CaO·SO_3	−7656	SO_2

Table 2
Composition of the raw meal fed to the raw mill (Taylor, 1990).

	wt%
Calcite	72.5
Quartz	6.0
Pyrophyllite	9.0
Kaolinite	2.4
Goethite	1.8
Moisture	8.0
Sulphur	0.3
Total	**100.0**

Table 3
Comparison of Bogue equation approximation and the simulation results.

Mineral	Bogue calculation [wt%]	Simulation [wt%]
Alite (C_3S)	60.6	60.4
Belite (C_2S)	17.5	17.2
Tricalcium aluminate (C_3A)	11.0	10.9
Tetracalcium aluminate (C_4AF)	8.6	8.2
Free CaO	0.0	0.0
CaO·SO3	2.3	2.5
Ash	0.0	0.8
Total	**100.0**	**100.0**

materials and the clinkerization stages (Taylor, 1990). Given the raw meal composition in Table 2, the approximate chemical composition of the four main clinker phases, C_3S, C_2S, C_3A, and C_4AF, can be estimated by Bogue equation (Bogue, 1929).

$$C_3S = 4.0710CaO - 7.6024SiO_2 - 6.7187Al_2O_3 - 1.4297Fe_2O_3 \quad (1)$$

$$C_2S = -3.0710CaO + 8.6024SiO_2 + 5.06383Al_2O_3 + 1.0785Fe_2O_3 \quad (2)$$

$$C_3A = 2.6504Al_2O_3 - 1.6920Fe_2O_3 \quad (3)$$

$$C_4AF = 3.0432Fe_2O_3 \quad (4)$$

The simulated clinker compositions are in good agreement with those estimated by the Bogue equation as shown in Table 3. It is assumed that 30% of sulphur in the raw material reacts with oxygen to become SO_2 in the first preheater and then leave the plant via the raw mill. The remaining sulphur is converted into SO_2 in the pre-calciner and subsequently all the SO_2 formed reacts with CaO and oxygen to form $CaO{\cdot}SO_3$ in the pre-calciner which is included in the clinker product (IEA, 2008).

The raw meal having 8% moisture is dried passing the raw mill where it is heated by contacting the flue gas leaving the preheaters directly. The flue gas flowrate to be fed to the raw mill is determined such that both gas and solid streams leave the raw mill at around 110 °C. The gas stream, leaving the pre-calciner at 915 °C, is cleaned of the entrained fine particles passing the four cyclones in series comprising the preheater where it heats up the raw meal up to 760 °C as shown in Fig. 2(a). The solid removal efficiency is assumed to be 94%, 90%, 85% and 80%, respectively from the preheater stage 1–4 (Alsop et al., 2007). It should be noted that calcination and clay decomposition start to take place at the 4th preheater with the 10% for calcination and 30% for clay decomposition set in this study referring to the clinker phase diagram in Taylor (1990).

The preheated raw meal enters the pre-calciner where 90% of the remaining calcites are calcined and all clays are decomposed into their constituents, such as alumina, silica, and ferrite, at the operating temperature of 915 °C. As the calcination and clay decomposition reactions are all endothermic, the pre-calciner is supplied with the heat generated from coal combustion with the tertiary air heated up to 908 °C by the clinker cooler. The flue gas leaving the kiln at 1025 °C flows into the pre-calciner in order to lower the CO_2 partial pressure and supply an additional heat source for the endothermic reaction.

The rotary kiln, where cement clinker is produced by counter-current contact of the gas and solid streams, has been simulated in three separate units so that the temperature change along the length can be simulated. The first unit, corresponding to the solid feed end of the kiln, is simulated as a heat-exchanger to heat the solid stream from 915 °C to 1250 °C by its direct contact with the kiln gas flowing in the opposite direction. Subsequently, the temperature of the solid stream increases up to 1450 °C by fuel combustion with primary and secondary airs in the reactor (second unit) in order to calcine the remaining calcite and make all clinkerization reactions completed. Finally, the kiln product formed in the second unit is cooled to 1370 °C with the incoming secondary air at the solid product end (third unit) (see Supporting information – S1).

The kiln product is sent to the clinker cooler in which it is cooled to 60 °C by ambient air. Even though there is a potential to burn alternative fuels such as tyres and biomass fuels in

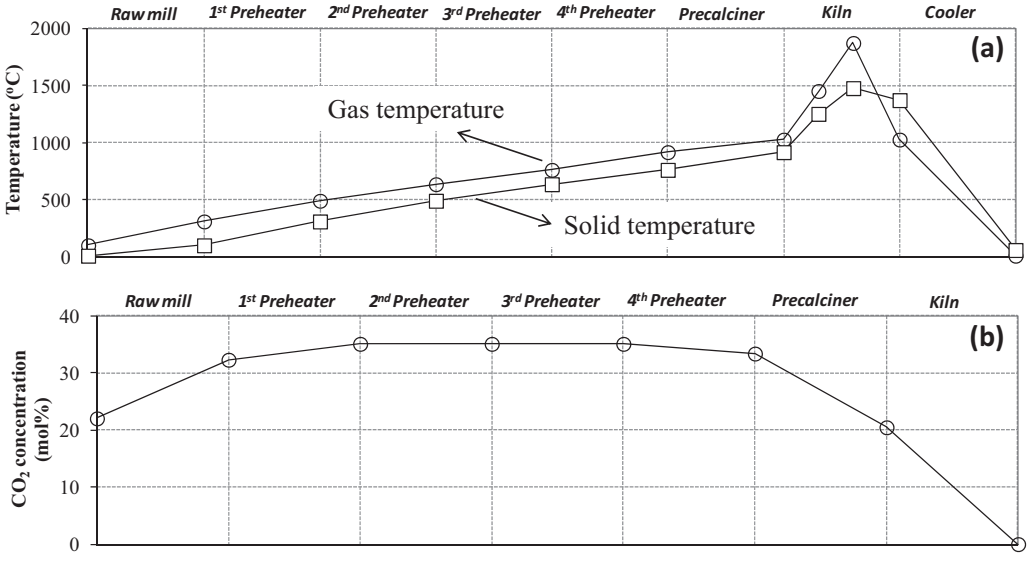

Fig. 2. Variations of (a) gas and solid temperatures and (b) CO_2 concentration along the cement plant.

Table 4
Composition of the fuels fed to the pre-calciner, kiln and calciner.

	Precalciner (coal[a]), wt%	Kiln (pet coke[a]), wt%	Calciner (pet coke), wt%
Carbon	64.4	85.6	87.2
Hydrogen	4.5	3.5	3.6
Nitrogen	1.4	1.8	1.8
Sulfur	0.9	5.3	3.6
Ash	12.1	0.2	0.2
Oxygen	7.2	1.8	1.8
Moisture	9.5	1.8	1.8
Total	**100.0**	**100.0**	**100.0**

[a] Data from IEA (2008).

Table 5
Mass balance of the base case simulation [kg/s].

Mass in		Mass out	
Raw meal	52.41	Clinker	31.61
Air	99.55	Flue gas	
Fuel		From fuel drying	4.30
Wet coal to pre-calciner	2.26	From raw mill	75.49
Wet pet-coke to kiln	1.18	Excess Air	44.00
Total in	155.40	Total out	155.40

the pre-calciner, coal is selected as a heat provider following the reference (IEA, 2008). The high temperature requirement in the kiln restricts the fuel flexibility; therefore, pet coke with low ash content is generally combusted in this reactor. Both fuel streams are dried completely by the hot flue gases from preheater. The excess air ratio is set as 10% to guarantee complete combustion in both reactors. The compositions of the fuels used in this study has been constructed from IEA (2008) report and presented in Table 4.

Tables 5 and 6 show the mass and heat balance around the cement plant obtained by the base case simulation. Given the raw meal composition, 1.66 kg/s of raw meal are required to produce 1 kg/s of clinker. The CO_2 generation intensity is around 0.8 ton CO_2/ton clinker that is within the range of 0.65–0.92 ton CO_2/ton cement given as the average CO_2 intensity for cement manufacture (IEA, 2007). Based on the heat balance, the required thermal energy for unit clinker production is estimated to be 3.13 MJ_{th}/kg clinker. The overall heat of chemical reactions involved in conversion of raw meal to clinker is estimated at about 178.4 GJ_{th}/h (1.57 MJ_{th}/kg clinker) by the difference between enthalpy in and out. The overall heat of reaction is lower in this simulation than in the reference (Taylor, 1990) (1.76 MJ_{th}/kg clinker) since it also takes into account the heat of the two highly exothermic reactions of sulphur conversion to SO_2 and its reaction with CaO.

3. Process simulation of a Ca-looping process

In all simulations, the operating condition of the carbonator is carefully chosen to capture 90% CO_2 from the feed gas and the $CaCO_3$ fed to the calciner is regenerated to CaO at complete conversion. The calciner temperature is selected to be 930 °C, which is higher than the pre-calciner temperature (915 °C), to guarantee complete calcination due to the CO_2 partial pressure in the calciner close to 1 atm. The temperature of the carbonator, which should be kept as close to the calciner temperature as possible in order to save the energy consumption for reheating the circulating solid, is fixed at 650 °C in this study.

The operating conditions inside the carbonator and the calciner are also favourable to the capture of SO_2 (Anthony et al., 1987). It is assumed that all SO_2 generated by combustion in the calciner is captured by CaO and the negative effects of sulphation on the maximum carbonation degree is taken into account in the carbonator model (Romano, 2012). As a result of the deterioration of the CO_2 absorption capacity through the carbonation/calcination cycles, fresh $CaCO_3$ needs to be added into the calciner while same amount of spent sorbents (CaO) on a molar basis are removed from the calciner. The $CaCO_3$ make-up, fuel, and oxygen streams fed to the calciner are neither preheated nor dried but directly fed to the calciner due to the lack of flue gas availability for preheating.

All the mathematical models for the carbonator have been solved in Matlab and then the carbonator unit was incorporated into the UniSim process simulation for a cement plant as a user defined operation. The Visual Basic code in a user defined operation transfers the input values from UniSim into the Matlab environment where the design calculations are implemented via a component object model (COM) interface. The calculated values are then sent back to Unisim and used for the mass and energy balance calculations in the complete process flowsheet. A detailed explanation of the mathematical models used for the carbonator unit can be found in Appendix A.

4. Process integration of a Ca-looping unit with a cement plant

One of the important issues while integrating a Ca-looping unit with a cement plant is the selection of a feed gas stream for the Ca-looping process. As the flue gas from pre-calciner flows through the process in the opposite direction to the solid flow for heat recovery, its temperature and CO_2 mole fraction varies over the process as shown in Fig. 2. Therefore, the optimal flue gas stream for the capture process should be selected taking into account the operating condition of a selected capture unit, ease of heat integration, and CO_2 partial pressure.

For the ease of retrofit, it can be envisaged that the flue gas stream after the raw mill and fuel drying would be an optimal feed for the capture unit. However, the flue gas at this location has

Table 6
Heat balance of the base case simulation [GJ_{th}/h].

Enthalpy in			Enthalpy out		
	Sensible heat	Heat by combustion[a]		Sensible heat	Heat of reaction
Raw meal	1.82		Clinker	5.12	
Air	3.25		Flue gas		
Fuel			From fuel drying	4.29	
Wet coal to pre-calciner	0.12	216.58	From raw Mill	72.95	
Wet pet-coke to kiln	0.05	139.25	Excess Air	45.77	
			Heat lost by radiation and convection	54.54	
			Overall heat of reaction		178.4 (1.57 MJ_{th}/kg)
Total in		**361.07**	**Total out**		**361.07**

The reference state for enthalpy is at 0 °C and 101 kPa.
[a] The heat by combustion of the fuel is a standard heat of combustion at 25 °C and 101 kPa.

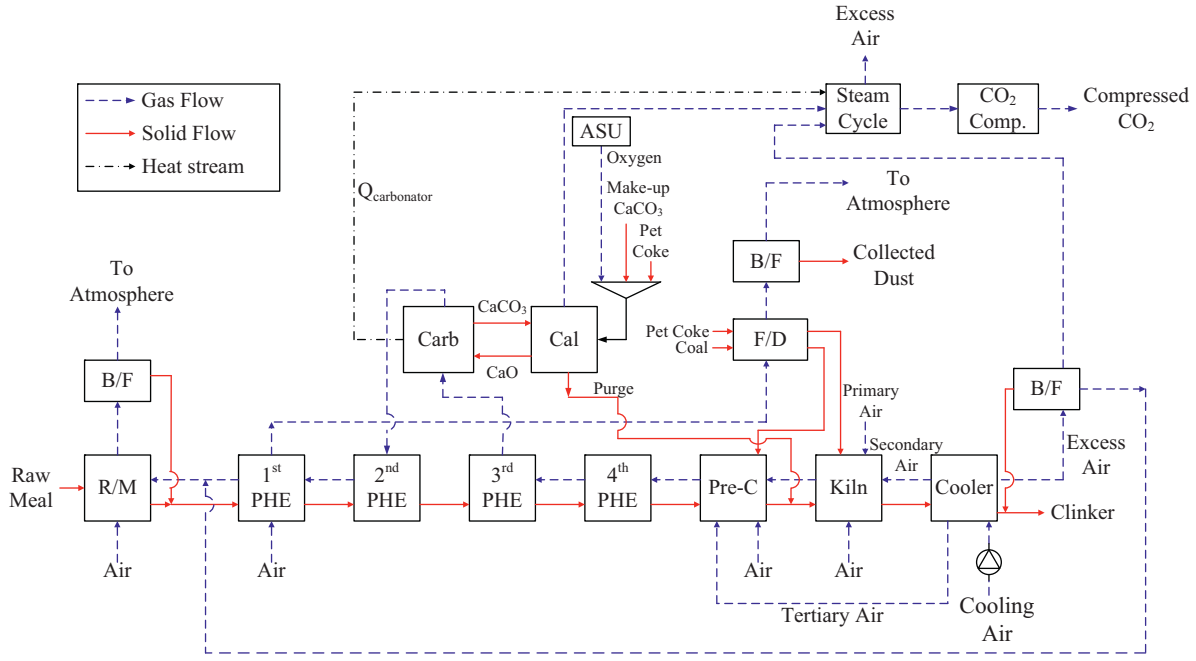

Fig. 3. Schematic diagram of the proposed process integration of a cement plant with a Ca-looping unit. Abbreviations: R/M, raw mill; B/F, bag filter; F/D, fuel drying; PHE, preheater; Pre-C, pre-calciner; Carb, carbonator; Calc, calciner; ASU, air separation unit; CO_2 Comp, CO_2 compression.

around 22 vol% CO_2 as shown in Fig. 2(b), which is the lowest value over the entire process. On the contrary, its volumetric flowrate is its highest at this point so a larger equipment size of the capture unit would be required. Furthermore, the flue gas may need to be reheated prior to being fed to the carbonator in order to initiate the carbonation reaction as the temperatures of the flue gases are around 110 °C. In addition, the heat of the CO_2-depleted gas from the carbonator needs to be recovered to improve the energy efficiency but an additional facility for heat recovery should be deployed for this purpose. In conclusion, the applications of Ca-looping processes to the end-of-the-pipe gas streams of the cement plants would require a complexity similar to those of power plants.

However, the flue gas at the exit of the 3rd preheater has a temperature of around 650 °C, as shown in Fig. 2(a), which is similar to the operating temperature of the carbonator. It indicates that the flue gas from the 3rd preheater would not require any pre-heating of the feed gas and would be preferable for the start-up of the carbonator. Moreover, there is no need to recover the heat from the CO_2-depleted flue gas stream for power generation and instead it is possible to return it back to the cement plant in order to heat up the raw materials in a similar way to the operation in the conventional cement plant. The flue gas at the 3rd preheater exit has a higher CO_2 concentration (~35 vol%) compared to the end-of-pipe stream (~22 vol%) as shown in Fig. 2(b) and, in proportion, such a lower gas flow rate would require a smaller carbonator size leading to lower capital expenditure. Therefore, a decision was made that the flue gas from the 3rd preheater stage is diverted to a Ca-looping unit for CO_2 capture as shown in Fig. 3. The CO_2-depleted flue gas from the carbonator is routed to the 2nd preheater stage for preheating the raw material further. It should be noted that it is still possible to capture CO_2 from all sources including calcination and fuel combustion with this configuration, which was initially proposed by ECRA (2007).

On the other hand, the CO_2 depleted flue gas flowing from the carbonator to the 2nd preheater would have a lower flowrate than that in the base case as a result of carbon capture and its heat duty is not large enough to heat the raw material up to a temperature that would be reached in the base case. Thus, part of the excess air from the clinker cooler as well as CO_2-depleted flue gas should be utilised for heating the raw material as shown in Fig. 3. In all cases of this study, the flowrate of excess air being sent to the raw mill was determined to heat the raw material entering the 1st preheater up to 110 °C. It should be noted that the clay components are not fed into the capture unit in this study as distinct from the reference (Rodriguez et al., 2012) since the sorbent performance has not been proven for this mixture yet and there would be a need of additional efforts for the circulation of inerts. As the purge stream of the Ca-looping unit is mixed with pre-calcined raw materials and then the mixture is sent to the kiln for clinker production, the mass and heat balance in the cement plant is significantly affected by changing the $CaCO_3$ make-up flow rate of the Ca-looping process. Firstly, since the CaO for clinkerization can be produced in the calciner as well as the pre-calciner, the ratio of calcite to clay in the raw meal should be decreased with an increasing F_0/F_{CO_2} in order to maintain the same clinker composition as that in the base case. Subsequently, the decreasing ratio of calcite to clay in the raw meal results in reduction in heat demand in the pre-calciner and, to a lesser extent, in the kiln.

In order to save the energy consumption for a Ca-looping process further, it is possible to recover the heat of reaction in the carbonator and the heat from the CO_2-rich stream and excess air. The heat of these hot streams can be recovered by way of generating steam for a steam cycle. The power generated can be utilised for the cement plant operation, the CO_2 compression unit, the air separation unit (ASU), etc. Since the solid removal efficiency is not 100% on the 3rd preheater stage, a new cyclone with higher efficiency has been included to prevent the solid transfer from the cement plant to the capture unit for the precise prediction of the carbonation efficiency in this unit. It is estimated that the additional pressure increment of the gaseous feed flowing to the carbonator would be approximately 0.16 bar. This would be sum of the pressure loss in operating the carbonator (pressure drop along the carbonator bed, 0.10 bar + gas injection through the nozzle, 0.03 bar) and the pressure drop relating to the additional cyclone (0.03 bar) (Alsop et al., 2007). 0.20 bar of a total pressure loss including a 25% safety margin is estimated. The boost of the gas stream pressure has been achieved

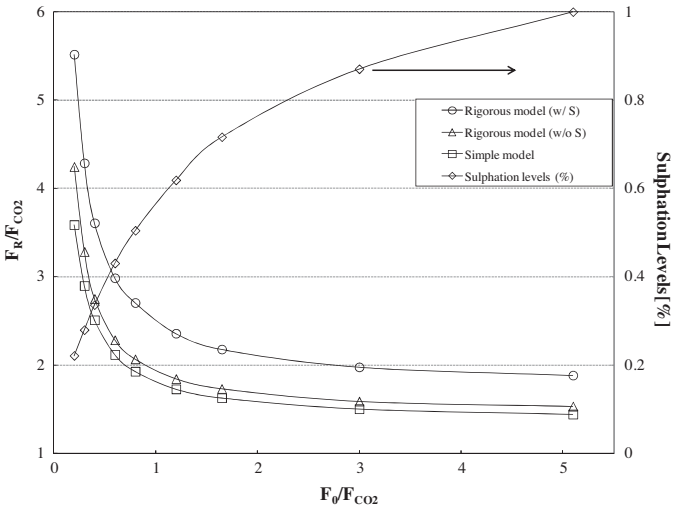

Fig. 4. Corresponding F_R/F_{CO_2} in range of F_0/F_{CO_2} ratio to reach 90% capture efficiency in the carbonator of proposed configuration (For the rigorous model, the carbonator temperature and pressure drop along the column were set as 650 °C and 0.1 bar, respectively while superficial velocity, u_0, was estimated to be 6 m/s. The sulphation level is shown at each F_0/F_{CO_2}).

by increasing the cooling air pressure flowing to the cement kiln. The ASU power consumption is set as 231 kWh per ton O_2 product at 99.5% oxygen purity (Marion et al., 2003). The CO_2 compression unit consists of a four-stage turbo compressor with intermediate cooling, followed by a pump once the CO_2 becomes a dense phase. The inlet temperature of each stage is fixed at 45 °C and the adiabatic efficiency of each compressor is assumed to be 75%. The power requirement for CO_2 compression up to 150 bar is estimated at 1.08 MJ_{th}/kg CO_2 using a 0.4 conversion factor of power to equivalent thermal energy. An example mass and energy balance calculations for the capture cases can be seen in Supporting Information – S2.

5. Results and discussion

Two mathematical models for the carbonator have been compared in this study as shown in Appendix A. While it is assumed that all the active fraction of CaO reacts with CO_2 in the feed gas in the 'simple model', the 'rigorous model' includes the effects of both hydrodynamics and reaction kinetics in the fluidised bed reactor. Moreover, the effects of sulphation on the maximum carbonation degree were taken into account in the rigorous model based on the experimental data of Piaseck for limestone sulphation up to 1% in each carbonation/calcinations cycle (Grasa et al., 2008a). Given a F_0/F_{CO_2}, the corresponding F_R/F_{CO_2} to achieve 90% CO_2 capture has been evaluated using the simple and rigorous models with results shown in Fig. 4. The minimum value of the F_0/F_{CO_2} being examined is set as 0.20 since the heat demand at the raw mill cannot be met even by employing the entire excess air in addition to the flue gas at a F_0/F_{CO_2} less than 0.20. The heat requirement in the raw mill keeps decreasing with increasing F_0/F_{CO_2} since the flowrate of raw meal into the raw mill decreases with an increase of the ratio. The upper limit of the F_0/F_{CO_2} ratio is determined as 5.10 since there is no calcite in the raw meal at this condition, that is to say, all the calcites in the feed are fed to the calciner. Therefore, the carbonator captures CO_2 generated only from the fuel combustion at this ratio. As shown in Fig. 4, it is clear that as the F_R/F_{CO_2} ratios estimated by the rigorous model using sulphur-free fuel are definitely higher than those by the simple model in range of the F_0/F_{CO_2} investigated. The extent of the difference between the two models is affected by the residence time of sorbents in the carbonator which

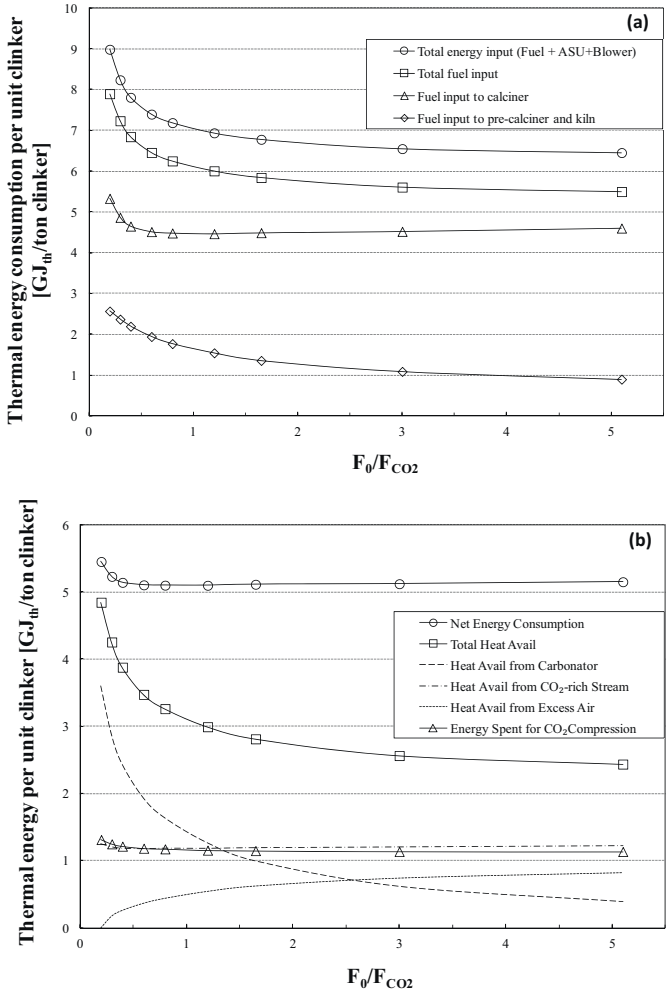

Fig. 5. (a) Energy consumption per unit clinker with respect to fuel and power and (b) net energy consumption per unit clinker considering heat recovery for power generation and CO_2 compression.

is determined by the amount of sorbent inventory in the reactor. However, when utilising the fuel having sulphur in the calciner, the required F_R/F_{CO_2} ratios need to be increased way above those with sulphur-free fuel since the CaO is significantly deactivated by sulphation. In this study the sulphur content in the fuel used in the calciner was adjusted so that the maximum sulphation, obtained at the 5.10 F_0/F_{CO_2} case can be 1%. It implies that the use of sulphur-free fuel would alleviate the severity of its operation condition due to the lower amount of solid circulation required given a F_0/F_{CO_2} ratio.

Fig. 5(a) shows the variation of the thermal energy requirement per unit clinker in terms of fuel combustion (pre-calciner, kiln, and calciner) and power consumption (ASU and blower) with the F_0/F_{CO_2}. The thermal requirement for the pre-calciner decreases with increasing F_0/F_{CO_2} as the heat requirement for the pre-calciner decreases in proportion to the reduction in calcite fed to the raw mill. The thermal requirement for the kiln has decreasing trends with the F_0/F_{CO_2} too since it is assumed that the calcite is completely calcined in the calciner while its conversion is only 90% in the pre-calciner. However, the reduction of energy demand in the kiln is not as significant as that in the pre-calciner because the solid flowrate to the kiln is almost constant regardless of the F_0/F_{CO_2} due to nearly constant clinker production rate in all cases. The heat requirement for the calciner shows a minimum over the F_0/F_{CO_2} range investigated. Before the minimum, it is decreasing due to decreasing

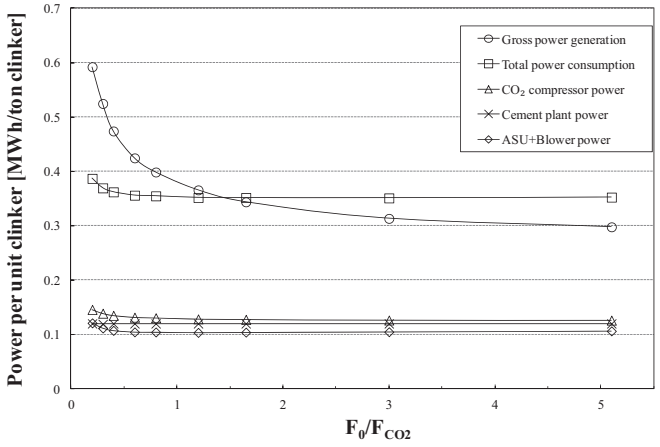

Fig. 6. Variation of power generation by heat recovery and power consumption with F_0/F_{CO_2} ratio.

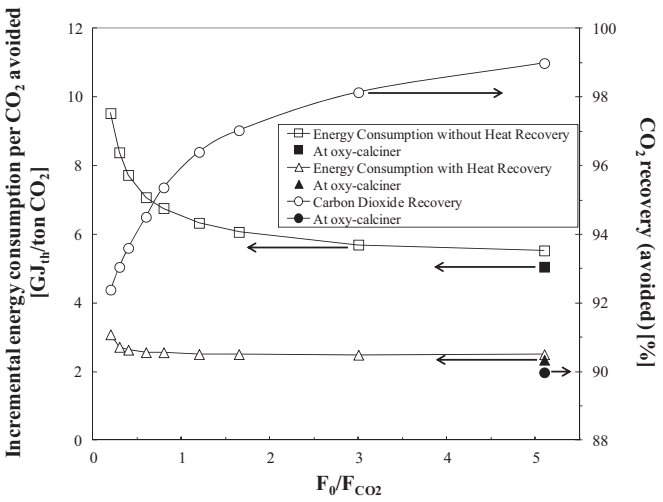

Fig. 7. Variation of CO_2 recovery based on CO_2 emission at base case and incremental energy consumption per CO_2 avoided with F_0/F_{CO_2} ratio.

circulating amount of solid, that is to say, the F_R/F_{CO_2} as shown in Fig. 4. However, after the minimum, the effect of the increase in the heat duty at the calciner caused by the F_0/F_{CO_2} increase dominates. The total fuel requirement shows a steady overall decrease with the increase of the F_0/F_{CO_2} ratio. The energy requirement for the ASU is proportional to the fuel consumption in the calciner and that for the cold air blower is constant with the F_0/F_{CO_2} ratio. The electric power consumptions in the ASU and blower are converted to their corresponding thermal energy consumption using a power plant efficiency of 0.4. This allows an overall comparison of different options in terms of the equivalent total thermal energy required. At least in terms of total thermal energy consumption for the fuel, the ASU and the blower it is preferable to operate a Ca-looping process at as high F_0/F_{CO_2} ratio as possible.

On the other hand, it is intuitively conceivable that a Ca-looping process can be made more efficient in terms of energy consumption if it is combined with a steam cycle for heat recovery. There are three different sources from which the heat can be recovered by generating steam and subsequently running a steam turbine. It is possible to generate steam by evaporating the water inside the carbonator in order to keep the reactor temperature constant at 650 °C and also recovering the heat from a CO_2-rich stream and the excess air as shown in Fig. 3. In case of heat recovery from the two gaseous streams, it is assumed that the hot gas can supply the steam cycle with thermal energy which is estimated as an enthalpy to be generated when cooled down to 150 °C. At 0.2 F_0/F_{CO_2}, as shown in Fig. 5(b), the heat that can be recovered in the carbonator is a maximum over the range due to the greatest heat of reaction generated in the carbonator and the largest amount of hot solids conveyed from calciner to carbonator (see Fig. 4). There is no heat to be recovered from the excess air since all the excess air should be diverted to the raw mill in order to compensate the deficiency of heat duty of the flue gas. Considering the energy consumption inclusive of CO_2 compression, the net energy consumption per unit clinker production is in the range of 5.2–5.5 GJ/ton clinker. This is equivalent to around 66% increase in energy consumption of a cement plant producing the same amount of clinker.

A simplified steam cycle design has been used to evaluate the power generation from the recovered heat. The turbine adiabatic efficiencies have been fixed at 86%, 86% and 95% for HP, IP and LP turbines, respectively (Ahn et al., 2013). With the proposed configuration (see Supporting information – S3) it is possible to estimate a lumped conversion factor of 0.44 which can be used to evaluate the electrical power generation from the total heat to be recovered from the cement plant integrated with the Ca-looping process. The total electricity generation ranges from 30 to 70 MWe and is shown in Fig. 6. It is predicted that the power generated in the steam cycle can exceed the power demand in the cement plant integrated with a Ca-looping process up to ~1.5 F_0/F_{CO_2}. The power use for the cement plant operation is assumed as 120 kWh/ton clinker (IEA, 2008; Taylor, 1990) regardless of the F_0/F_{CO_2}.

It should be noted that what is fixed in this study is not a CO_2 recovery in the overall cement process but a CO_2 recovery in the carbonator. As shown in Fig. 7 the percentage of CO_2 avoided is as low as 92% at 0.2 F_0/F_{CO_2} since most CO_2 is captured in the carbonator with 90% capture rate. It increases up to 99% at 5.10 F_0/F_{CO_2} because most CO_2 is captured with 100% CO_2 recovery in the calciner. In this study, the limiting case named 'oxy-calciner only' has been simulated without a carbonator. All calcites are calcined in the calciner separate from the pre-calciner in a similar way to the 5.10 F_0/F_{CO_2} case, but there is no carbon capture applied to the kiln gas. In this case, the percentage of CO_2 avoided is 90% since this process can capture CO_2 relating to calcinations and fuel combustion in the calciner, but cannot capture CO_2 generated by fuel combustion in the kiln with a loss of 9% in overall capture efficiency.

The incremental energy consumption per CO_2 avoided without heat recovery also shows decreasing trends with F_0/F_{CO_2} similarly to the total energy input per unit clinker in Fig. 5(a). It implies that it would be better to generate CaO by oxy-combustion rather than by the pre-calciner in the existing plant if no heat recovery system is added. The incremental energy consumption per CO_2 avoided at the 'oxy-calciner only' and 5.10 cases are 5.1 and 5.5 GJ_{th}/ton CO_2 avoided respectively without heat recovery. It is thought that the difference between the two cases (0.4 GJ/ton CO_2) can be explained by additional energy consumption resulting from circulating solids between the carbonator and the calciner. It was indicated that the thermal energy consumption in the MEA process when it is used for carbon capture from a cement plant (IEA, 2008) requires around 9.2 GJ_{th}/ton CO_2 avoided including its compression work. In this respect, even without heat recovery, the energy consumption at the 5.10 F_0/F_{CO_2} case is significantly lower than that for MEA process (IEA, 2008). With heat recovery put in place, the resulting energy consumption decreases further to 2.5 GJ_{th}/ton CO_2 avoided for the 5.10 case and 2.3 GJ_{th}/ton CO_2 avoided for the 'oxy-calciner' case. Table 7 shows the quantitative difference of fuel and power consumptions between the cement plant without capture and those integrated with Ca-looping units and heat recovery steam cycle at various F_0/F_{CO_2} conditions. Table 7 also includes the change of mass flow rates of limestones entering the plant through the raw mill and calciner with the value of F_0/F_{CO_2}. The proposed cement plants

Table 7
Detailed constituents of CO_2 avoided energy consumption considering heat recovery.

F_0/F_{CO_2}	Mass flow rates (kg/s)			ΔH[c]	ASU[c]	CO_2 compression[c]	Cold air blower[c]	Total[c]
	Clay	Limestone						
		Raw mill	Calciner					
0.2[a]		28.85	9.09	−0.24	1.30	1.75	0.15	2.96
0.3		25.57	12.37	−0.23	1.18	1.65	0.15	2.75
0.4		22.82	15.12	−0.22	1.12	1.59	0.15	2.64
0.6		18.70	19.24	−0.20	1.07	1.54	0.15	2.56
0.8	10.28	15.67	22.27	−0.16	1.06	1.51	0.15	2.56
1.2		11.81	26.13	−0.15	1.04	1.47	0.15	2.51
1.65		8.62	29.32	−0.13	1.04	1.45	0.14	2.50
3.0		4.02	33.92	−0.11	1.04	1.42	0.14	2.49
5.1[b]		0	37.94	−0.09	1.04	1.41	0.14	2.50
Oxy		0	37.94	−0.08	1.05	1.37	–	2.34

[a] The lower limit was defined as the heat requirement in the raw mill cannot be met below this point
[b] The upper limit was defined as no calcite is fed to the raw mill at this F_0/F_{CO_2} and more calcite would be fed to the cement plant through the oxy-calciner than required above this point.
[c] Unit: GJ_{th}/ton CO_2 avoided.

integrated with Ca-looping units are designed with a steam cycle that can recover heat contained in the hot excess air which would be lost in the conventional cement plant. As a result the net thermal energy consumption in the cement plants with Ca-looping units is always lower than that in the conventional cement plant as shown in Table 7. It is clear that it would be extremely inefficient to operate a Ca-looping unit at low F_0/F_{CO_2} ratio without heat recovery but CO_2 can be recovered with almost constant energy consumption regardless of the F_0/F_{CO_2} ratio if a proper heat recovery is deployed. Moreover, the electricity required to operate a cement plant integrated with a Ca-looping process can be generated in situ by a steam cycle attached to the capture unit without any external source of electricity which would be associated with carbon emissions.

6. Conclusions

A way of capturing CO_2 from cement plants by integrating it with a Ca-looping process has been investigated. The cement process simulation implemented in this study was proven to be reliable in that the total energy consumption estimated by the simulation lies within the range of those reported in the literature and the clinker compositions estimated in the simulation are in good agreement with those calculated by the Bogue equation. Among the flue gas streams, the gas stream leaving the 3rd preheater was selected to be the optimal feed suitable for the Ca-looping capture unit since (1) it does not have to be preheated, (2) it has a higher CO_2 partial pressure and a lower total volumetric flowrate, and (3) a simpler design of the steam cycle for heat recovery is possible.

The upper and lower limits of the F_0/F_{CO_2} ratio have been set in this study in order to see the effect of F_0/F_{CO_2} on the energy consumption. Given 90% carbon capture in the carbonator, the CO_2 avoided in the overall integrated process ranges from 92% to 99% depending on the F_0/F_{CO_2} ratio. The incremental energy consumption by carbon capture decreases with the F_0/F_{CO_2} ratio but, with heat recovery from the capture unit, the energy consumption can be almost constant regardless of the ratio.

It should be noted that there may be a constraint in the minimum fuel supply to the kiln to ensure a stable operation in the kiln as pointed out in the IEA study (2008). Therefore, the actual upper limit of the F_0/F_{CO_2} ratio needs to be defined considering plant operability. Moreover, the estimation of the amount of heat that can be recovered from three high temperature sources can be made more accurate by inclusion of a detailed steam cycle in the integrated process flowsheet.

Acknowledgements

The authors acknowledge financial support from Turkish Ministry of Education and EPSRC S&I Award (EP/F034520/1).

Appendix A. Carbonator design

In the simple model, the maximum average carbonation degree of sorbent in the solid population is defined as Eq. (A1) (Abanades, 2002) where $X_{max,N}$ is maximum carbonation degree after N cycles of carbonation/calcination in Eq. (A2) (Grasa and Abanades, 2006) and r_N is mass fraction of particles calculated from mass balance in Eq. (A3) (Abanades, 2002). The CO_2 capture efficiency in the carbonator (E_{CO_2}) is defined as Eq. (A4).

$$X_{max,ave} = \sum_{N=1}^{N=\infty} r_N X_{max,N} \tag{A1}$$

$$X_{max,N} = \frac{1}{1/(1-X_r)+kN} + X_r \tag{A2}$$

$$r_N = \frac{F_0 F_R^{N-1}}{(F_0+F_R)^N} \tag{A3}$$

$$E_{CO_2} = \frac{F_R X_{max,ave}}{F_{CO_2}} \tag{A4}$$

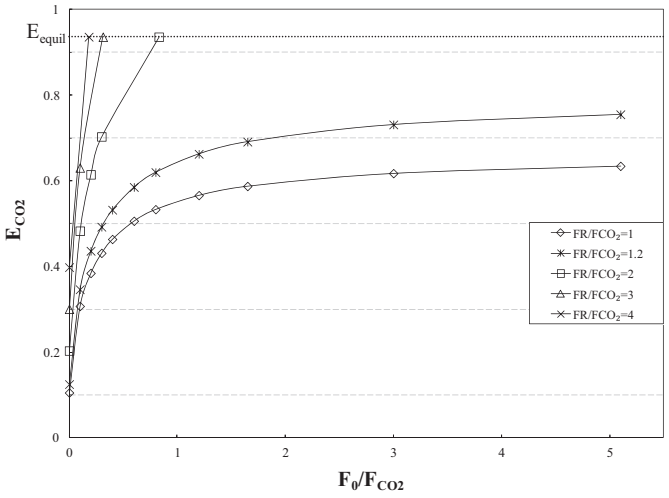

Fig. 8. Graphical explanation of Eq. (A5) at 650 °C (k = 0.66 and X_r = 0.0969).

X_r and k are constants specific to the type of limestone. For non-sulfated Piaseck limestone the values of the constants are $k = 0.66$ and $X_r = 0.0969$ (Romano, 2012; Grasa et al., 2008a). The capture efficiency calculated from this model is shown in Fig. 8. The maximum carbonation efficiency is also limited by the equilibrium of CO_2 over CaO as shown in Eq. (A5) (Garcia-Labiano et al., 2002). The equilibrium at 650 °C is shown as a horizontal dotted line in Fig. 8.

$$P_{CO_2,eq} = 4.137 \times 10^{12} \ \exp\left(-\frac{20474}{T}\right) \tag{A5}$$

The target is to achieve 90% carbon capture in the carbonator. As it can be noticed from Fig. 8, various sets of F_0/F_{CO_2} and F_R/F_{CO_2} can provide capture efficiency of 90% according to Eqs. (A1)–(A4). However, an advanced carbonator model is necessary in order to deal with the hydrodynamics of a fluidized bed system. Detailed carbonator designs have been investigated including the design of a bubbling fluidized bed (Abanades et al., 2004) and a fast fluidized bed (Romano, 2012; Lasheras et al., 2011). Therefore, in this study, the detailed circulating fluidized bed (CFB) model for fast fluidization has been employed based on the approach proposed in the literature (Romano, 2012; Rampinelli, 2010) and named rigorous model in this study. This model is briefly described here but further details can be found in the literature (Romano, 2012).

The particle distribution part of the rigorous model has been based on the Kunii–Levenspiel model for CFBs (Kunii and Levenspiel, 1991), and the reactor is divided into two sections, a lower dense region and an upper lean region. To calculate the values of H_l (height of the upper lean region) and $\varepsilon_{s,e}$ (exiting solid fraction), the particle distribution equations (Eqs. (A6) and (A7)) need to be solved simultaneously.

$$\varepsilon_{s,e} = \varepsilon_S^* + (\varepsilon_{s,d} - \varepsilon_s^*)e^{-aH_l} \tag{A6}$$

$$\frac{W_s}{A_t \rho_s} = \frac{(\varepsilon_{s,d} - \varepsilon_{s,e})}{a} + H_t \varepsilon_{s,d} - H_l(\varepsilon_{s,d} - \varepsilon_s^*) \tag{A7}$$

The solution of the gas phase material balance in the CFB which can be rearranged with the first order kinetic law for the carbonation reaction (Grasa et al., 2008b) leads to two final equations, (A8) and (A9) which give CO_2 concentrations at the top of the dense region ($C_{CO_2,d}$) and at the reactor exit ($C_{CO_2,out}$), respectively.

$$C_{CO_2,d} = C_{CO_2,eq} + (C_{CO_2,in} - C_{CO_2,eq}) \times e^{-[\xi\varepsilon_{s,c}\delta k_{ri,ave} + 1/((1/\delta K_{cw}) + 1/(\xi\varepsilon_{s,w}(1-\delta)k_{ri,ave}))]H_d/u_o} \tag{A8}$$

$$C_{CO_2,out} = C_{CO_2,eq} + (C_{CO_2,d} - C_{CO_2,eq})e^{-(k_{ri,ave}/u_O)(x+y)} \tag{A9}$$

$$x = \xi\varepsilon_s^* \left[H_l - \frac{1-\eta_{sd}}{b}(1 - e^{-bH_l})\right] \tag{A10}$$

$$y = \xi(\varepsilon_{s,d} - \varepsilon_s^*) \left[\frac{1 - e^{-aH_l}}{a} - \frac{1-\eta_{sd}}{a+b}(1 - e^{-(a+b)H_l})\right] \tag{A11}$$

The average kinetic constant ($k_{ri,ave}$) and volume fraction of potentially active solids (ξ) should be known initially to solve Eqs. (A8) and (A9). Therefore, as another approach, the considerations of solid composition in the carbonator, probability density function (f_t), i.e. the fraction of particles with certain residence times, in Eqs. (A12)–(A14) and the distribution of the particle based on the number of carbonation–calcination cycles as given in Eq. (A3) allows the calculation of the average carbonation level, X_{ave} (Eq. (A15)) as well as $k_{ri,ave}$ (Eq. (A16)) and ξ.

$$f_t = \frac{1}{\tau} e^{-(t/\tau)} \tag{A12}$$

$$\tau = \frac{n_{s,a}}{F_R} \tag{A13}$$

$$n_{s,a} = \frac{W_s}{M_s}(1 - x_{ash} - x_{CaSO_4}) \tag{A14}$$

$$X_{ave} = \sum_{N=1}^{+\infty} \left(\int_0^{t_{lim}} f_t X(t, N, C_{CO_2}^*) dt + \int_{t_{lim}}^{\infty} f_t X_{max,N} dt \right) \tag{A15}$$

$$k_{ri,ave} = \frac{\rho_{s,a}}{M_{s,a}} \sum_{N=1}^{+\infty} r_N \int_0^{t_{lim}} f_t k_s S_N (1 - X(t, N, C_{CO_2}^*))^{2/3} dt \tag{A16}$$

It should be noted that, the effect of sulphation on the maximum carbonation degree in the rigorous model was considered by adjusting the k and X_r constants (Eq. (A2)) corresponding to the sulphation level of Piaseck limestone (Romano, 2012; Grasa et al., 2008a). The given equations are only valid up to a sulphation level of 1%.

$$\Delta X_{CaSO_4} = \frac{F_S}{F_R + F_0} \tag{A17}$$

$$k = 0.026 \times (\Delta X_{CaSO_4} \times 100)^2 + 0.219 \times (\Delta X_{CaSO_4}) + 0.660, \quad 0 \le \Delta X_{CaSO_4} \le 0.01 \tag{A18}$$

$$X_r = (-0.1118 \times \Delta X_{CaSO_4} \times 100) + 0.0969, \quad 0 \le \Delta X_{CaSO_4} \le 0.005 \tag{A19}$$

$$X_r = (-0.0298 \times \Delta X_{CaSO_4} \times 100) + 0.0559, \quad 0.005 \le \Delta X_{CaSO_4} \le 0.001 \tag{A20}$$

The capture efficiency can be calculated by two different ways, Eqs. (A21) and (A22).

$$E'_{CO_2} = \frac{F_R X_{ave}}{F_{CO_2}} \tag{A21}$$

$$E''_{CO_2} = \frac{F_{CO_2} - V_{g,out} C_{CO_2,out}}{F_{CO_2}} = \frac{V_{g,in} C_{CO_2,in} - V_{g,out} C_{CO_2,out}}{V_{g,in} C_{CO_2,in}} \tag{A22}$$

The values for the variables required for the carbonator calculation are imported from the cement plant simulation via a COM interface (F_{CO_2}, F_0, F_R, F_{ash}, F_S, u_0, d_p, T, M_s, p, μ, $C_{CO_2,in}$, $V_{g,in}$, W_s, H_t, x_{CaSO_4}, x_{ash}). The area of the reactor (A_t), average solid density (ρ_s) and average molar mass values (M_s) are initially calculated. By assuming a CO_2 concentration inside the carbonator ($C_{CO_2}^*$), X_{ave} is obtained using Eqs. (A12)–(A15) and the first capture efficiency, E'_{CO_2} is calculated using Eq. (A21). The length of dense and lean regions is determined by Eqs. (A6)–(A7), given the total height of carbonator, H_t. The average kinetic constant of the carbonation reaction, $k_{ri,ave}$, can be calculated using (A16) with the same $C_{CO_2}^*$ used in the E'_{CO_2} calculation. Using the $k_{ri,ave}$, the CO_2 concentration at the outlet is calculated by Eqs. (A8)–(A11). Finally the second capture efficiency, E''_{CO_2} can be obtained using Eq. (A22). An iterative calculation is applied to obtain same capture efficiency from the two different methods. Once the same capture efficiency is reached, it is possible to calculate a new A_t using the average value of inlet and outlet flowrates and a new M_s based on the X_{ave}. Based on the new A_t and M_s, the new $C_{CO_2}^*$ needs to be calculated to give same capture efficiency, i.e. another iterative loop is set to obtain A_t and M_s outside the iterative loop for $C_{CO_2}^*$. The parameters used in the calculations can be found in the literature (Romano, 2012).

Appendix B. Supplementary data

Supplementary material related to this article can be found, in the online version, at doi:10.1016/j.ijggc.2013.10.009.

References

Abanades, J.C., 2002. The maximum capture efficiency of CO_2 using a carbonation/calcination cycle of $CaO/CaCO_3$. Chemical Engineering Journal 90, 303–306.

Abanades, J.C., Anthony, E.J.D., Lu, D.Y., Salvador, C., 2004. Capture of CO_2 from combustion gases in a fluidized bed of CaO. AIChE Journal 50 (7), 1614–1622.

Ahn, H., Luberti, M., Liu, Z., Brandani, S., 2013. Process configuration studies of the amine capture process for coal-fired power plants. International Journal of Greenhouse Gas Control 16, 29–40.

Alonso, M., Rodríguez, N., González, B., Grasa, G., Murillo, R., Abanades, J.C., 2010. Carbon dioxide capture from combustion flue gases with a calcium oxide chemical loop. Experimental results and process development. International Journal of Greenhouse Gas Control 4, 167–173.

Alsop, P.A., Chen, H., Tseng, H., 2007. The Cement Plant Operations Handbook. Tradeship Publications Ltd, Surrey, UK.

Anthony, E.J., Becker, H.A., Code, R.W., McCleave, R.W., Stephenson, J.R., 1987. Bubbling fluidized bed combustion of syncrude coke. In: Presented at the International Conference on Fluidized Bed Combustion, Boston, MA.

Arias, B., Diego, M.E., Abanades, J.C., Lorenzo, M., Diaz, L., Martinez, D., Alvarez, J., Sanchez-Biezma, A., 2013. Demonstration of steady state CO_2 capture in a 1.7 MWth calcium looping pilot. International Journal of Greenhouse Gas Control 18, 237–245.

Bogue, R.H., 1929. Calculation of the compounds in Portland cement. Industrial & Engineering Chemistry Analytical Edition 1 (4), 192–197.

Bosoaga, A., Masek, O., Oakey, J.E., 2009. CO_2 capture technologies for cement industry. Energy Procedia 1 (1), 133–140.

Charitos, A., Hawthorne, C., Bidwe, A.R., Sivalingam, S., Schuster, A., Spliethoff, H., Scheffknecht, G., 2010. Parametric investigation of the calcium looping process for CO_2 capture in a 10 kW_{th} dual fluidized bed. International Journal of Greenhouse Gas Control 4, 776–784.

Curran, G.P., Fink, C.E., Gorin, E., 1967. Carbon dioxide-acceptor gasification process: studies of acceptor properties. Advanced Chemistry Services 69, 141–165.

CW Group, 2012. Global Cement Volume Forecast Report.

Dean, C.C., Blamey, J., Florin, N.H., Al-Jeboori, M.J., Fennell, P.S., 2011a. The calcium looping cycle for CO_2 capture from power generation, cement manufacture and hydrogen production. Chemical Engineering Research and Design 89 (6), 836–855.

Dean, C.C., Dugwell, D., Fennell, P.S., 2011b. Investigation into potential synergy between power generation, cement manufacture and CO_2 abatement using the calcium looping cycle. Energy & Environmental Science 4, 2050–2053.

Dieter, H., Hawthorne, C., Bidwe, A.R., Zieba, M., Scheffknecht, G., 2012. The 200 kWth dual fluidized bed calcium looping pilot plant for efficient CO2 capture: plant operating experiences and results. Naples, Italy. Proceeding of the 21st International Conference on Fluidized Bed Combustion, 397–404.

Dong, R.F., Lu, H.F., Yu, Y.S., Zhang, Z.X., 2012. A feasible process for simultaneous removal of CO_2, SO_2 and NO_x in the cement industry by NH_3 scrubbing. Applied Energy 97, 185–191.

ECRA, 2007. Technical Report: Carbon Capture Technology – Options and Potentials for the Cement Industry.

ECRA, 2009. Technical Report: ECRA CCS Project – Report about Phase II.

Garcia-Labiano, F., Abad, A., de Diego, L.F., Gayan, P., Adanez, J., 2002. Calcination of calcium-based sorbents at pressure in a broad range of CO_2 concentrations. Chemical Engineering Science 57, 2381–2393.

Grasa, G.S., Abanades, J.C., 2006. CO_2 capture capacity of CaO in long series of carbonation/calcination cycles. Industrial & Engineering Chemistry Research 45, 8846–8851.

Grasa, G.S., Alonso, M., Abanades, J.C., 2008a. Sulphation of CaO particles in a carbonation/calcination loop to capture CO_2. Industrial & Engineering Chemistry Research 47, 1630–1635.

Grasa, G.S., Abanades, J.C., Alonso, M., Gonzales, B., 2008b. Reactivity of highly cycled particles of CaO in a carbonation/calcination loop. Chemical Engineering Journal 137, 561–567.

Handagama, N.B., Kotdawala, R.R., Vajpeyi, A., 2013. Heat integration of a cement manufacturing plant with an absorption based carbon dioxide capture process, Publication No. US20130074695 A1.

Hasanbeigi, A., Price, L., Lin, E., 2012. Emerging energy-efficiency and CO_2 emission-reduction technologies for cement and concrete production: a technical review. Renewable and Sustainable Energy Reviews 16, 6220–6238.

Hassan, S.M.N., 2005. Techno-economic study of CO_2 capture process for cement plants. Chemical Engineering, University of Waterloo, Canada (Masters Thesis).

IEA, 2007. Tracking Industrial Energy Efficiency and CO_2 emissions. OECD/IEA, Paris.

IEA, 2008. CO_2 Capture in the Cement Industry, July 2008/3.

IEA, 2009. Carbon Emission Reductions up to 2050. In: Cement Technology Roadmap 2009.

IEA Clean Coal Center, 2011. CO_2 abatement in the cement industry.

Kunii, D., Levenspiel, O., 1991. Fluidization Engineering, second ed. Butterworth-Heinemann, Boston.

Lasheras, A., Strohle, J., Galloy, A., Epple, B., 2011. Carbonate looping process simulation using a 1D fluidized bed model for the carbonator. International Journal of Greenhouse Gas Control 5 (4), 686–693.

Marion, J.L., Bozzuto, C.R., Nsakala, N.Y., Liljedahl, G.N., Andrus, H.E., Chamberland, R.P., 2003. Greenhouse Gas Emissions Control By Oxygen Firing In Circulating Fluidized Bed Boilers: Phase 1 – a Preliminary Systems Evaluation. Alstom Power Inc. and National Energy Technology Laboratory, US Department of Energy.

Martínez, I., Murillo, R., Grasa, G., Abanades, J.C., 2011. Integration of a Ca-looping system for CO_2 capture in existing power plants. AIChE Journal 57, 2599–2607.

Pan, X., Clodic, D., Toubassy, J., 2013. CO_2 capture by antisublimation process and its technical economic analysis. Greenhouse Gases: Science and Technology 3 (1), 8–20.

Plötz, S., Bayrak, A., Galloy, A., Kremer, J., Orth, M., Wieczorek, M., Ströhle, J., Epple, B., 2012. First carbonate looping experiments with a 1 MWth test facility consisting of two interconnected CFBs. In: 21st International Conference on Fluidized Bed Combustion, Naples, Italy, pp. 421–428.

Rampinelli, G., 2010. Modello matematico di un reattore per la cattura della CO_2 post-combustione tramite ossido di calico. Politecnico di Milano, Italy (Masters Thesis).

Rodriguez, N., Alonso, M., Abanades, J.C., Grasa, G., Murillo, R., 2009. Analysis of a process to capture the CO_2 resulting for pre-calcination of the limestone feed to a cement plant. Energy Procedia 1, 141–148.

Rodríguez, N., Murillo, R., Alonso, M., Martinez, I., Grasa, G., Abanades, J.C., 2011a. Analysis of a process for capturing the CO_2 resulting for pre-calcination of limestone in a cement plant. Industrial & Engineering Chemistry Research 50 (4), 2126–2132.

Rodríguez, N., Alonso, M., Abanades, J.C., 2011b. Experimental investigation of a circulating fluidized-bed reactor to capture CO_2 with CaO. AIChE Journal 57, 1356–1366.

Rodriguez, N., Murillo, R., Abanades, J.C., 2012. CO_2 capture from cement plants using oxyfired precalcination and/or calcium looping. Environmental Science & Technology 46 (4), 2460–2466.

Romano, M.C., 2012. Modelling the carbonator of a Ca-looping process for CO_2 capture from power plant flue gas. Chemical Engineering Science 69 (1), 257–269.

Romeo, L.M., Catalina, D., Lisbona, P., Lara, Y., Martínez, A., 2011. Reduction of greenhouse gas emissions by integration of cement plants, power plants, and CO_2 capture systems. Greenhouse Gases: Science and Technology 1, 72–82.

Shimizu, T., Hirama, T., Hosoda, H., Kitano, K., Inagaki, M., Tejima, K., 1999. A twin fluid-bed reactor for removal of CO_2 from combustion processes. Chemical Engineering Research & Design 77 (A1), 62–68.

Stallmann, O., 2013. Integrated carbon dioxide capture for cement plants, Publication No. WO/2013/024340.

Strohle, J., Galloy, A., Epple, B., 2009. Feasibility study on the carbonate looping process for post-combustion CO_2 capture from coal-fired power plants. Energy Procedia 1, 1313–1320.

Taylor, H.F.W., 1990. Cement Chemistry. Academic Press Ltd., New York.

Vera, E.R.M., 2009. Method for capturing CO_2 produced by cement plants by using the calcium cycle, Publication No. US20090255444 A1.

WBCSD, 2009. Cement Industry and CO_2 Performance. Getting the Numbers Right. Cement Sustainability Initiative, Geneva.

WWF, 2008. Blueprint for the Cement Industry: How to Turn Around the Trend of Cement Related Emissions in the Developing World.

Zhao, M., Andrew, I.M., Harris, T., 2013. Review of techno-economic models for the retrofitting of conventional pulverised-coal power plants for post-combustion capture (PCC) of CO_2. Energy & Environmental Science 6, 25–40.